

THE FERMI FEL2 ELECTRO OPTICAL SAMPLING DESIGN AND OPERATIONAL EXPERIENCE

M. Veronese*, A. Abrami, E. Allaria, M. Bossi, P. Cinquegrana, M. Danailov, A. Demidovich, G. Gaio, S. Grulja, G. Pangon, G. Penco, P. Sigalotti, C. Spezzani, M. Trovò, M. Tudor
Elettra Sincrotrone Trieste, Basovizza, Italy

Abstract

This paper reports on the design and operational experience of an electro optical sampling (EOS) diagnostics based on the same femtosecond laser used for the seeding process of the FERMI FEL2. This design allows operating in parallel with the FEL2, minimizing time jitter with respect to the seed laser which is the main time marker of the FEL process by removing the time jitter contributions related to the use of an external laser. In our setup a fraction of the energy from the seed laser amplifier is extracted and delivered via a dedicated low vacuum transport system to the EOS setup in the tunnel with beam pointing stabilization actively obtained by piezo actuators. The laser beam size, pulse compression management, polarization cleaning and selection are performed in the tunnel prior to injecting the laser beam in the vacuum chamber. The spatial decoding scheme is employed, with a 100 micron thick GaP crystal and a detection performed in cross polarizers setup using a CMOS camera. The EOS has been characterized in terms of temporal resolution, jitter and drift. Finally, its capability to operate as longitudinal feedback system is also reported.

INTRODUCTION

The FERMI FEL has the peculiar characteristics to be a seeded FEL [1]. This means that the bunching at the origin of the FEL amplification process is generated by a UV fs laser overlapped in time and space with the electron beam. The energy modulation that is imposed on the electron beam is converted in longitudinal charge modulation by a dispersive section. The temporal properties of the FERMI FEL are hence phase locked with the seed laser. Using a fraction of the seed laser beam for an Electro Optical Sampling (EOS) it is possible to achieve electron beam profile measurements locked with the seed laser timing. In this way one aims at obtaining better performances in terms of temporal jitter and drift compared to using an external laser.

FEL LAYOUT

FERMI is a seeded FEL based on the high gain harmonic generation (HG) scheme [2]. Two FEL lines, FEL-1 and FEL-2, are presently installed at the facility. FEL-1 is a single stage seeded FEL generating coherent light in the 65-20 nm wavelength range. FEL-2 is a double stage seeded FEL based on the fresh bunch injection technique [3], where the additional stage extends the spectral

range to 20-4 nm. At FERMI the electron bunch is generated at 10 Hz by a photo-injector GUN with energy of 5 MeV. The electrons are accelerated by an S-band linac. The bunch length can be manipulated by means of a magnetic bunch compressor chicane (BC1). The microbunching present in the bunch can be mitigated before BC1 by a laser heater (LH) system. The final energy is up to 1.5 GeV in FEL operative conditions. After the acceleration, the electrons are injected into one of the two FEL lines (either FEL-1 or FEL-2).

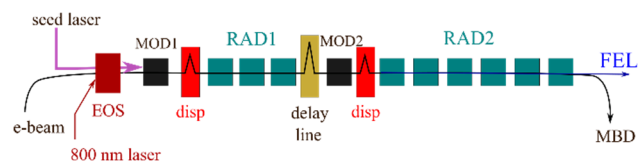


Figure 1: Layout of the FERMI FEL-2.

The EOS diagnostics, as shown in Fig. 1, has been installed in the FEL-2 line, close to the interaction point of the seed laser with the electrons, just before the first modulator of the first stage of FEL-2.

EOS DESIGN

Concept

The EOS beam instrumentation described in this paper is based on the spatial decoding scheme [4]. In such a design the laser passes the EO crystal at an angle and the position of the beam induced birefringence on the crystal maps the relative timing of the electron beam with respect to the laser.

Source

The laser pulses for the EOS are extracted just outside the IR amplifier (800 nm) in the seed laser optical table located in the SLR room. The main beam travels to the OPA and is converted to UV in the range 238–267 nm [5] and transported in low vacuum from the SLR room to the undulator hall injection point. The EOS beam is instead directed to another low vacuum transport that brings it to the EOS optical table located in the undulator room just before the first modulator undulator, as depicted in Fig. 2. The IR beam used for EOS has an initial energy of about 100 μ J, a pulse duration of about 350 fs and a diameter of 8 mm.

Transport

The transport consists of a low vacuum line equipped with low GDD mirrors. There are two remotely controllable beam steering points. The first in the SLR optical table

* email address: marco.veronese@elettra.eu

while the second is in the EOS optical table. Both are equipped with a motorized kinematic mirror for coarse adjustment and a piezo platform for beam position stabilization. The rest of the mirrors are located in low vacuum chambers and are rarely operated. The first part of the transport is located in the SLR room, the beam is then steered to the adjacent UTDR room, through the vertical penetration that transverse the 2.5 m thick concrete floor separating the ground level from the undulator hall tunnel and then arrives on the EOS optical table. The total length of the transport from the extraction point to the optical table is of 29.5 meters. The laser safety of the transport is guaranteed by vacuum sensors, position sensor on the enclosure covers, beam shutters and controlled by the FERMI laser safety PLC. The vacuum level is kept at a few mbar and is usually operated in static vacuum to minimize pump induced vibrations.

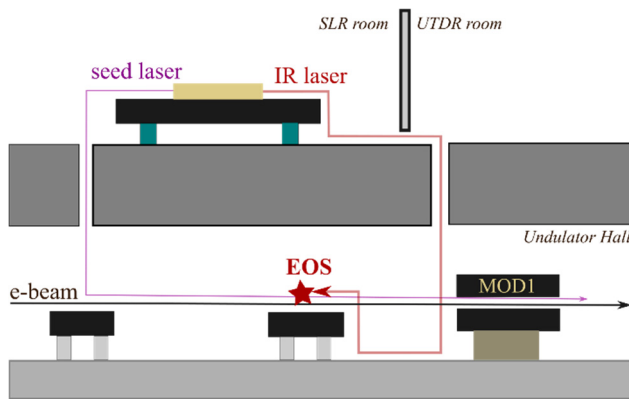


Figure 2: Layout of the EOS laser vacuum transport.

Optical Table Setup

The optical table setup is depicted in Fig. 3. It is equipped with several mirrors to accommodate enough path length to allow the correct temporal overlap of the electron beam with the EOS laser. A fraction of the energy passing the 1st mirror is used as the target of the CCD1 camera. The beam polarization is set by the first polarizer P1 before reaching the 2nd steering device which, as the 1st steering device, is also a mirror mounted on a piezo platform installed in a motorized kinematic mount. The beam is then delivered to an optical delay line with 200 mm travel needed for the fine temporal overlap. The beam path continues passing through a compressor in Littrow configuration base on a pair of Ibsen transmission gratings with 1250 lines/mm that is used to compress the laser pulses to about 50 fs duration. The beam is steered by mirror and again a small fraction of the incident energy is transmitted to a screen imaged by the camera CCD2. This is the sensor of the 2nd steering device which guarantees trajectory stabilization of the table optical transport which is 8.2 m long. The laser beam then passed a motorized zero order half wave plate, then a thin film polarizer. In this way a variable attenuator is obtained and it is used to control the intensity of the beam on the EO crystal. The following element is a 50/50 beam splitter that reflects half of the energy to a diagnostics setup and transmit 50 % towards the EO vacuum chamber. In the diagnostic setup we can have either an

online energy measurement or an online IR single shot autocorrelation. This device makes use of a Fresnel biprism and a Lasertec type I BBO crystal 0.2 mm thick, coupled to a Basler acA1300-75gm camera (CCD3), equipped with a 400 nm bandpass filter. Downstream of the beam splitter, a calcite Glan polarizer is used to clean the polarization to increase the extinction ratio of the measurement. After that a motorized zero order waveplate is used to set the wanted polarization direction. A final cylindrical lens with $f=300$ mm is used to focus the laser beam on the vertical direction. After passing a periscope the laser reaches the EO crystal inside the vacuum chamber with a small vertical beam size. The EOS crystal is a 100 μ m thick GaP. The vacuum chamber is depicted in Fig. 4. by geometrical construction the beam is expected to pass at 3 mm distance from the edge of the GaP crystal.

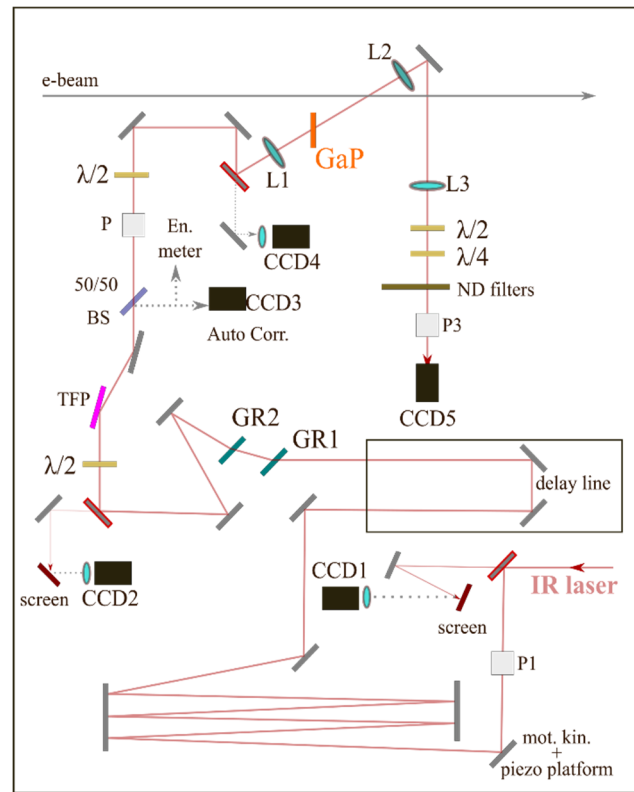


Figure 3: Optical scheme of the EOS table setup.

After the EO crystal the laser is extracted from the vacuum chamber. Lenses L2 and L3 provide the imaging of the crystal on to a Basler AcA1300-75gm camera called CCD5. The intensity is adjusted by ND filters mounted on a remotely controller filter wheel. The polarization analysis is provided by a zero order $\lambda/2$ waveplate and a $\lambda/4$ waveplate followed by a calcite Glan polarizer. They are set in near extinction configuration to obtain the best signal to background ratio.

The above describes our implementation of the so called spatial decoding scheme [5]. We use a 30 deg incidence angle of the laser on the EO crystal to optimize the phase matching of the laser and the electron beam induced birefringence as they travel through the GaP crystal. Camera CCD4 is used in conjunction with the 1st $\lambda/2$ to achieve

long term stabilization of the energy reaching the GaP crystal.

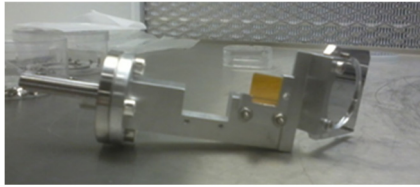


Figure 4: GaP crystal.

MEASUREMENTS

When there is no temporal coincidence of electron beam and laser, CCD5 images a quite broad spot. When there is coincidence, the EO signal appears as brighter area on the broad spot. The horizontal axis of the image corresponds to the temporal axis. To better discriminate the EOS signal, a background image without coincidence is subtracted from images. Figure 5 shows an example of two images with and without background subtraction.

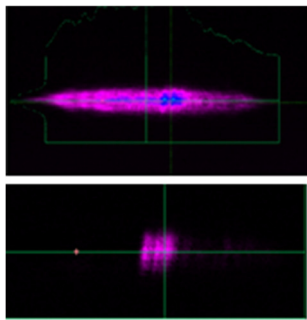


Figure 5: CCD5 image: without background subtraction (top) and with background subtraction (bottom).

The image can be vertically summed to obtain a profile. In Fig. 6 we show a series of such profiles. As Fermi operates at 50 Hz it is possible to tag the images and the profiles with a bunch number and correlate them to other machine parameters of interest.

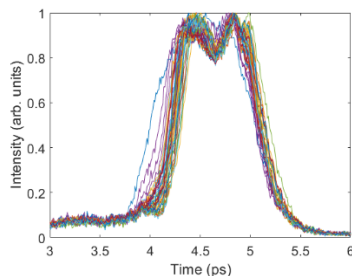


Figure 6: EOS bunch profiles (50 shots).

The centroid of the profile is taken as measurement of the electron beam arrival. This information is also used in the calibration process: the laser is temporally shifted with a delay line and the EO signal shifts horizontally on the background spot. Through this scan it is possible to characterize the temporal acquisition window of EOS as is shown in Fig. 7.

The EOS signal profile, as per [6], is the result of the convolution of several frequency depended functions, such

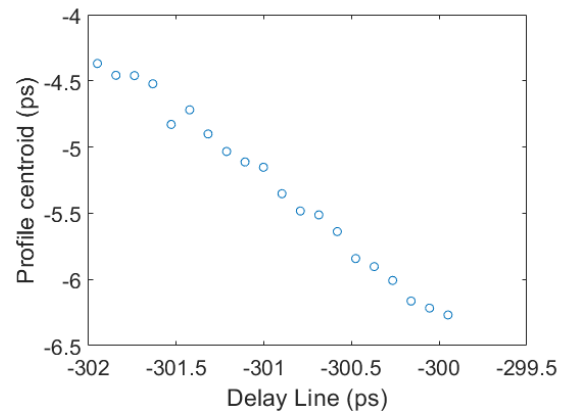


Figure 7: image profile vs delay line position.

as the crystal EO coefficient $r_{41}(\omega)$, the index of refraction $n(\omega)$, its thickness, the electron bunch profile Fourier transform $F_e(p(t))$ and the laser profile Fourier transform $F_l(p(t))$. For our setup the main temporal resolution limitations are expected to derive mostly from GaP phononic resonances and thickness effects. From analysis of the EOS signal profiles we get an overall estimate of the resolution around 110 fs, well suited for our 1 ps long electron bunches. The instrumentation has been tested as sensor of a longitudinal feedback, to stabilize the FEL signal and recover in case of time drifts. Figure 8 shows a test of such feedback. In this case a temporal shift of 2.3 ps was imposed deliberately by imposing a trajectory target change in the BC01 bunch compressor. This switched off completely the FEL as no temporal overlap of electron beam and seed laser was present anymore. Then the EOS based feedback was turned on and quickly the FEL signal was recovered.

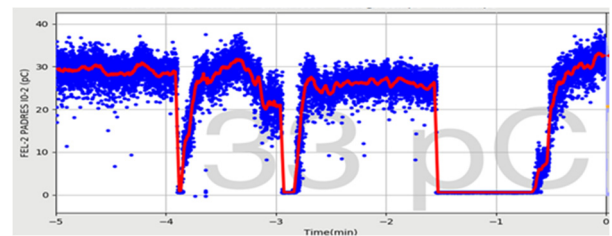


Figure 8: FEL-2 intensity during test of EOS based temporal feedback.

CONCLUSION

The paper describes the design and the operational experience of the EOS instrumentation installed in the FEL-2 line of FERMI FEL. The concept of using the seed laser as EO probe laser to have a phase locked EOS measurement has been successfully tested.

REFERENCES

- [1] L. H. Yu, "Generation of intense uv radiation by subharmonically seeded single-pass free-electron lasers", *Phys. Rev. A*, vol. 44, pp. 5178–5193, 1991.
doi:10.1103/PhysRevA.44.5178
- [2] E. Allaria *et al.*, "Highly coherent and stable pulses from the FERMI seeded free-electron laser in the extreme ultraviolet",

Nat. Phot., vol. 6, p. 233, 2012.

doi:10.1038/nphoton.2012.233

- [3] E. Allaria *et al.*, “Tunability experiments at the FERMI@ Elettra free-electron laser”, *New J. Phys.*, vol. 14, pp. 113009, 2012. doi:10.1088/1367-2630/14/11/113009

- [4] A. L. Cavalieri *et al.*, “Clocking Femtosecond X Rays”, *Phys. Rev. Lett.*, vol. 94, pp. 114801, 2005. doi:10.1103/PhysRevLett.94.114801

- [5] P. Cinquegrana *et al.*, “The seed laser system of the FERMI free-electron laser: design, performance and near future upgrades”, *High Power Laser Sci. Eng.* vol. 9, pp. e61, 2021. doi:10.1017/hpl.2021.49

- [6] S. Casalbuoni *et al.*, “Numerical studies on the electro-optic detection of femtosecond electron bunches”, *Phys. Rev. ST Accel. Beams*, vol. 11, pp. 072802, 2008. doi:10.1103/PhysRevSTAB.11.072802